

Study of EM waves in Periodic Structures: Photonic Crystals and Negative refraction

Massachusetts Institute of Technology
6.635 lecture notes

1 Introduction

In the previous class, we have introduced various concepts necessary for the study of EM waves in photonic crystal structures. We shall now use these concepts to explain various results such as:

- Reconstruction of the permittivity profile.
- The band diagrams for rectangular and triangular lattices.
- k -surfaces for various eigenvalues.

In particular, we will show an example of how a periodic structure can exhibit k -surfaces typical of a negative refraction material (the concept of k -surface for left-handed materials was first introduced in the class of February 24, 2003).

This class is based on the following two references::

- [1] C. Luo, S. G. Johnson, and J. D. Joannopoulos, “*All-angle negative refraction without negative effective index*”, Physical Review B, vol. 65, 2002, #201104.
- [2] J. D. Joannopoulos, R. D. Meade, and J. N. Winn, “*Photonic Crystals, Molding the Flow of Light*”, Princeton University Press, 1995.

2 Retrieving the permittivity

We have presented already the way to calculate the Fourier coefficients of the permittivity for cylindrical inclusions, with circular cross-section (see section 5 of March 19 2003 notes). An example was also given in Fig. 7. We shall just briefly comment on this.

It is known already that a photonic crystal is defined by a lattice (rectangular, triangular, . . .) and a basis (the shape of the inclusion). Both have to be incorporated in the retrieval of ϵ for example. In the treatment presented last time (section 5 of the reference mentioned above) we obtained the Fourier coefficients of the permittivity for a specific lattice (square). The result was:

$$\tilde{\epsilon}(G_\rho) = \begin{cases} \epsilon_a f_r + \epsilon_b (1 - f_r) & \text{if } G_\rho = 0 \\ (\epsilon_a - \epsilon_b) f_r \frac{2J_1(G_\rho R_c)}{G_\rho R_c} & \text{elsewhere.} \end{cases} \quad (1)$$

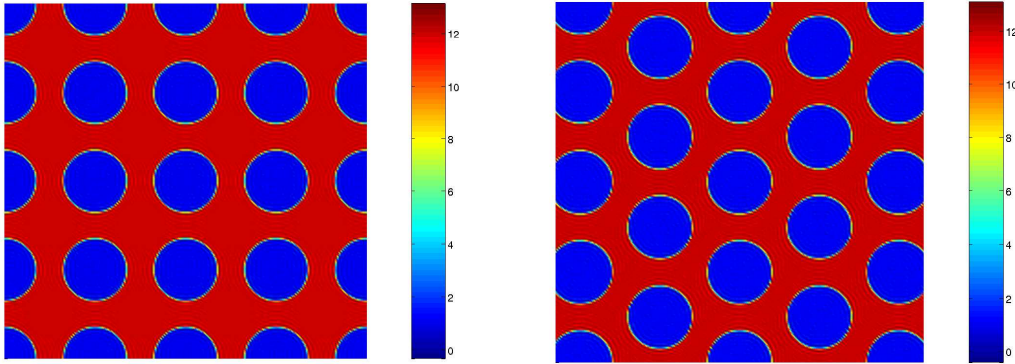
Yet, the information on the basis is also included in Eq. (1), since both G_ρ and f_r will depend on it.

It is straightforward to show that:

☞ Square lattice: $f_r = \pi \left(\frac{R_c}{a}\right)^2$ (where R_c is the radius of the inclusions and a the lattice constant).

☞ Triangular lattice: $f_r = \frac{2\pi}{\sqrt{3}} \left(\frac{R_c}{a}\right)^2$.

An illustration for square and triangular lattices is given in Fig. 1 (note that since the permittivity is obtained from its Fourier coefficients, a unavoidable Gibbs phenomenon will occur).



(a) Square lattice ($f_r = 38.48\%$).

(b) Triangular lattice ($f_r = 44.43\%$).

Figure 1: Reconstruction of the permittivity for cylindrical rods of circular cross-section for (a) a square lattice and (b) a rectangular lattice. Other parameters are: $\epsilon_a = 1$, $\epsilon_b = 12$, $R_c/a = 0.35$.

3 Band diagrams

The purpose of all the mathematical developments presented so far (getting the Fourier coefficients of the permittivity, building the eigensystem, etc) is to eventually obtain the eigenvalues and eigenvectors of the problem. Eigenvalues correspond to dispersion diagrams whereas eigenvectors correspond to the actual field distributions. We shall limit ourselves here to the consideration of eigenvalues only.

Upon solving the eigensystem:

$$\Theta \bar{H}(\bar{r}) = \left(\frac{\omega_k}{c} \right)^2 \bar{H}(\bar{r}), \quad (2a)$$

$$\Theta = \nabla \times \left[\frac{1}{\epsilon(\bar{r})} \nabla \times \right], \quad (2b)$$

(with the condition $\nabla \cdot \bar{H}(\bar{r}) = 0$ to reduce the size of the system), we get a set of eigenvalues for each incident \bar{k} . The band diagrams are then constructed by sweeping *all possible* \bar{k} .

Because of the periodicity of the medium the “*all possible*” \bar{k} can be reduced to the first Brillouin zone and, by symmetry, further reduced to the irreducible Brillouin zone. In addition, as we have seen, it is also enough to span the edge of the Brillouin zone since it corresponds to the maximum diffraction condition. Again by symmetry, we further reduce the domain to the edge of the irreducible Brillouin zone.

This zone will of course depend on the lattice, as is shown in Figs 2 and 3 of the March 19 2003 notes. For both cases, the irreducible Brillouin zone is depicted in Fig. 2.

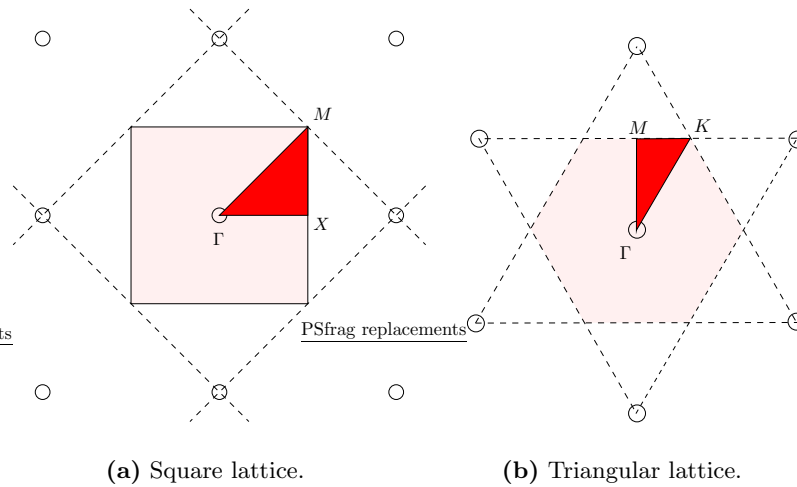


Figure 2: Irreducible Brillouin zones (red region) for (a) a square lattice and (b) a triangular lattice. Each region is defined between symmetry points of the crystal.

In order to span the edge of the irreducible Brillouin zone, we therefore need to know the coordinates of the symmetry points of the crystal. It is easy to show that:

- Square lattice:

$$\Gamma \rightarrow (k_x = 0, k_y = 0), \quad (3a)$$

$$X \rightarrow (k_x = \frac{\pi}{a}, k_y = 0), \quad (3b)$$

$$M \rightarrow (k_x = \frac{\pi}{a}, k_y = \frac{\pi}{a}). \quad (3c)$$

- Triangular lattice:

$$\Gamma \rightarrow (k_x = 0, k_y = 0), \quad (4a)$$

$$K \rightarrow (k_x = \frac{2\pi}{3a}, k_y = \frac{2\pi}{\sqrt{3}a}), \quad (4b)$$

$$M \rightarrow (k_x = 0, k_y = \frac{2\pi}{\sqrt{3}a}). \quad (4c)$$

Having these limit points, we can sweep \bar{k} , solve the eigensystem and obtain the eigenvalues. An example is given in Fig. 3.

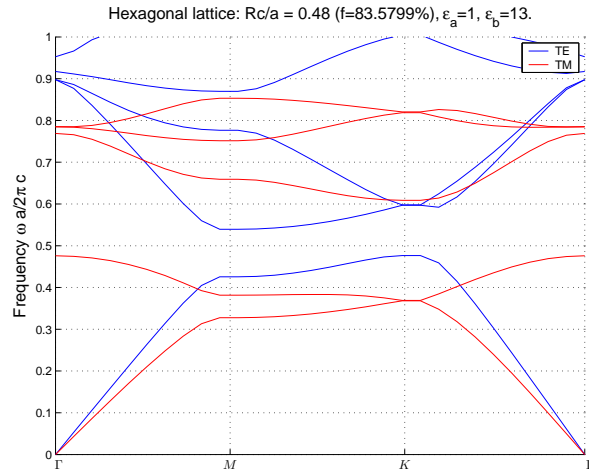
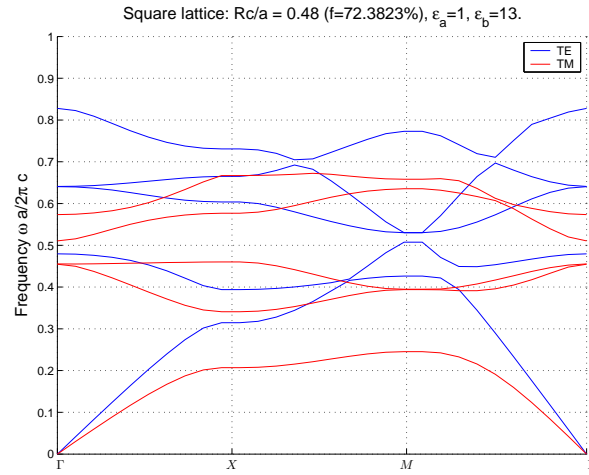


Figure 3: Band diagram for TE and TM modes as function of the normalized frequency for (a) a square lattice and (b) a triangular lattice. Notice the absolute band gap for TM modes. Parameters are: $\epsilon_a = 1$, $\epsilon_b = 13$, $R_c/a = 0.48$. *Important note:* TE modes are here defined as transverse to the axis of the crystal (z axis), therefore with an in-plane electric field!! Note also that these curves have not yet fully reached convergence.

4 *k*-surfaces

4.1 Well-chosen example

We can generalize the band diagram of the previous section (which, again, spans only the edge of the Brillouin zone), to the entire zone or even to the entire photonic crystal.

The example we shall consider from now on is taken from [1] and the parameters are summarized in Tab. 1. In addition, we shall work with TE modes (remember that in this notation, TE corresponds to an in-plane electric field).

Lattice:	square
Inclusions:	$\epsilon_a = 1$
Background:	$\epsilon_b = 12$
Radius :	$R_c/a = 0.35$

Table 1: Parameters for our example [1].

The band diagram obtained for this case is depicted in Fig. 4.

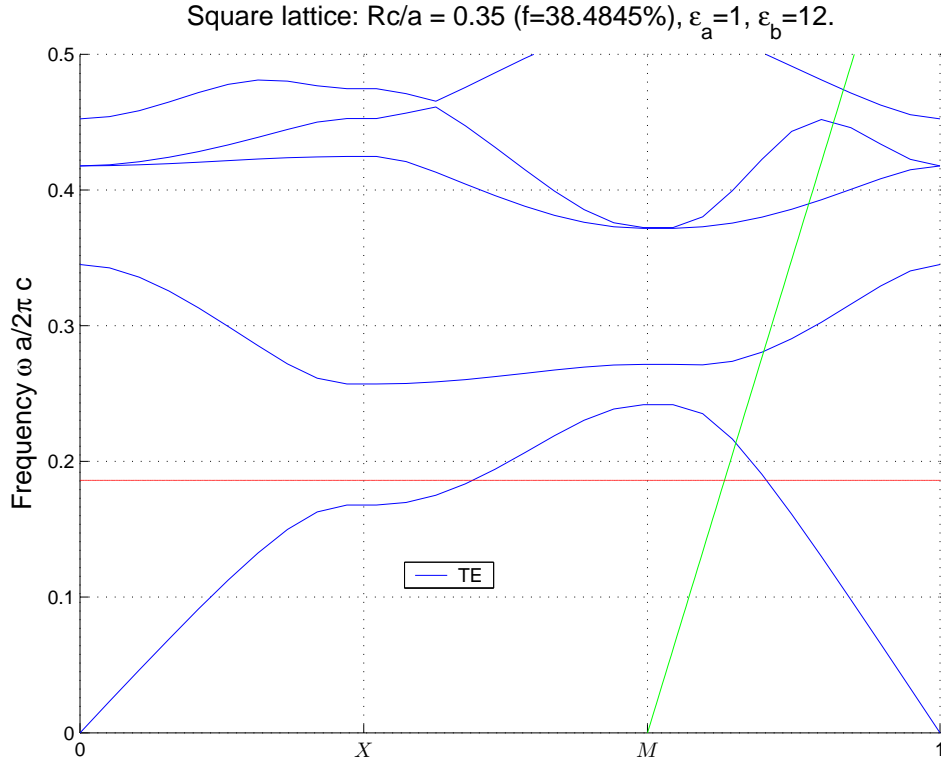


Figure 4: Band diagram for TE modes for the structure defined in Tab. 1. The horizontal line is at the frequency corresponding to a change of curvature of the *k*-surface, and the green line is the light-line shifted to M.

We can also extend the plot from the edge of the irreducible Brillouin zone to the entire structure, for various eigenstates. This is represented in Figs. 5 to 7.

4.2 Negative refraction

From the k -surfaces shown in the figures of this section, we see that there is the potential of negative refraction (the iso-frequency surfaces converge to a point as frequency increases). Yet, we need to make sure that:

1. We can couple to one of these surfaces from free-space.
2. The power is bending on the same side of the normal.

Answer to both points is shown in Fig. 4.

1. Light-line: the light-line gives the radius of the k -surface of an EM wave impinging on the crystal from free-space. In order to have a possible coupling, whole (or part) of the free-space k -surface has to be included in one of the k -surfaces of the crystal. The light-line is represented in Fig. 4 by the green line (it is actually the translation of the light-line to M). Its intersection with say the curve of the first eigenvalue gives the maximal frequency for which the condition mentioned above (total inclusion of the free-space k -surface into a k -surface of the crystal) is satisfied.

Note also that in order to have a negative refraction, the free-space k -surface has to be included in one of the k -surfaces converging to M and therefore, the actual crystal needs to be rotated by 45° .

2. Power bending: around M , the power is converging to a single point when frequency is increased. Yet, the direction of the power can be deduced from the gradient of the k -curves and therefore, directly from their radius of curvature. Hence, if the radius of curvature is such that the gradient is pointing toward M , the refraction will be negative.

The frequency at which the radius of curvature diverge is given by the horizontal line in Fig. 4, which can be obtained by a direct inspection of Fig. 5(c).

As it can be seen, the power can bend on the opposite side of the normal. However, the phase is still propagating forward, which justifies the title of the paper: “*All-angle negative refraction without negative index*”.

We can also examine the second eigenvalue and see if a similar phenomenon can appear. The k -surface has been depicted in Fig. 6(b) and is shown again in Fig. 9 with less curves represented. It is clear from this figure that again, there is a point at which the radius of curvature of the k -curves changes, and energy converges to a single point (Γ this time) as frequency increases. It is therefore again possible to have a negative index of refraction. Notice that in this case

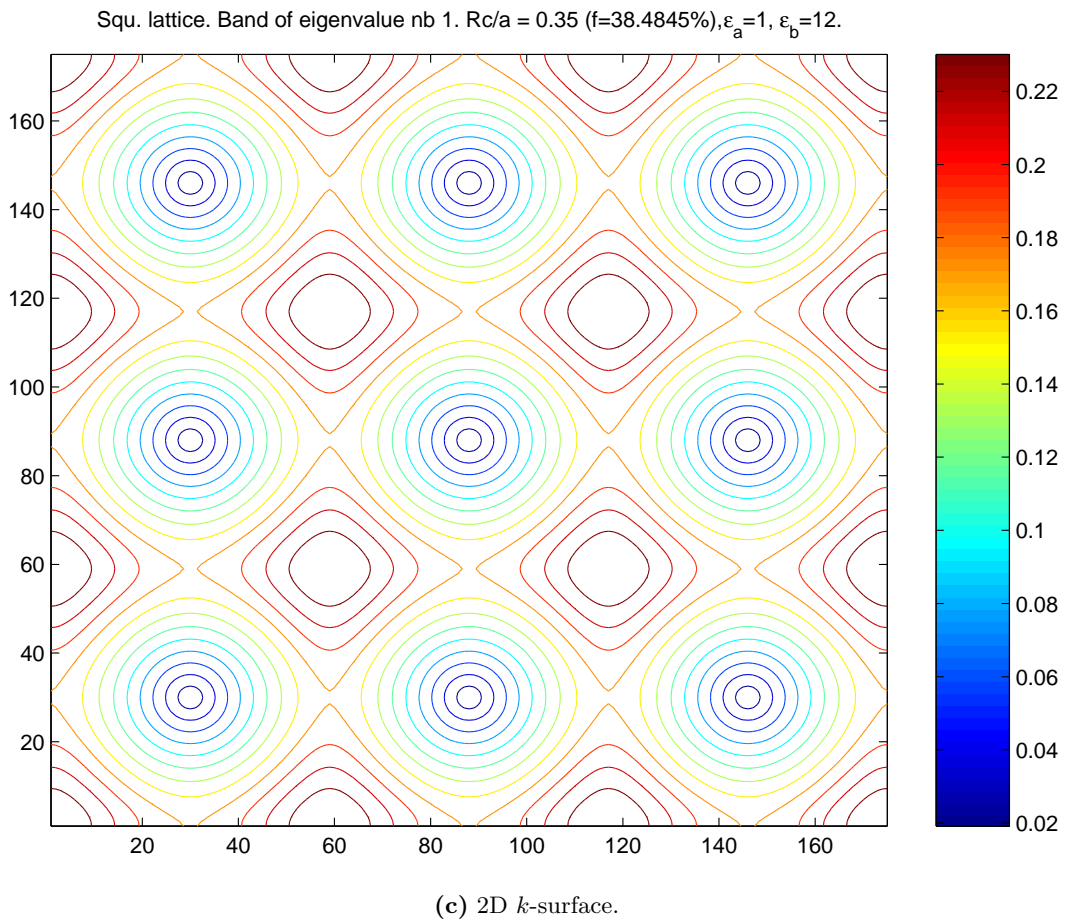
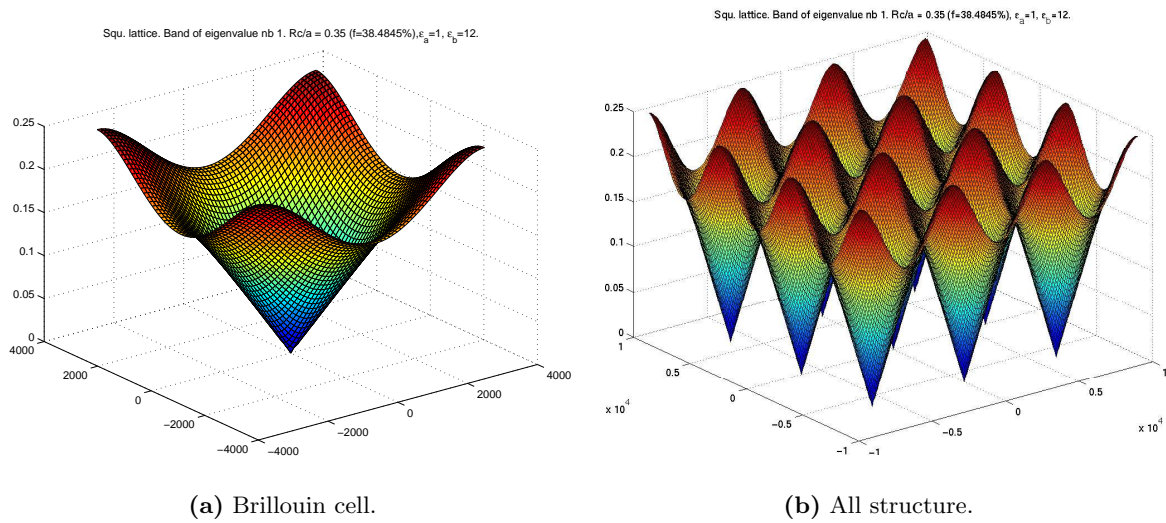
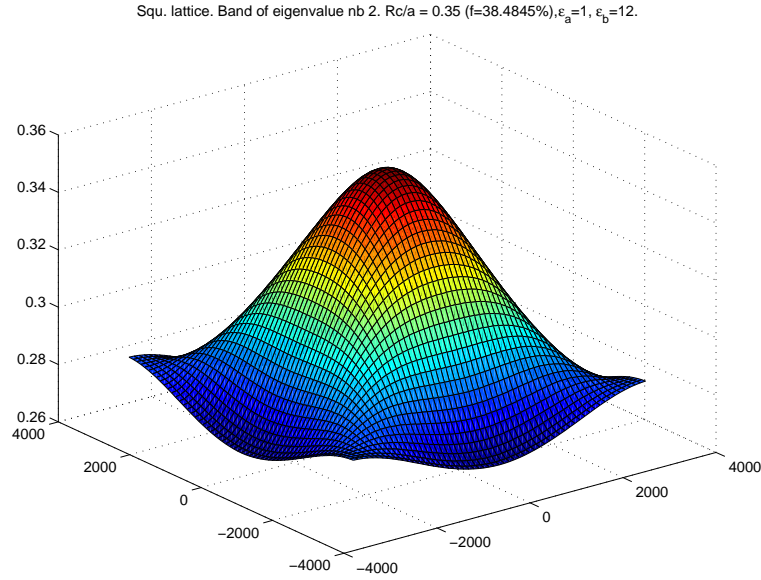
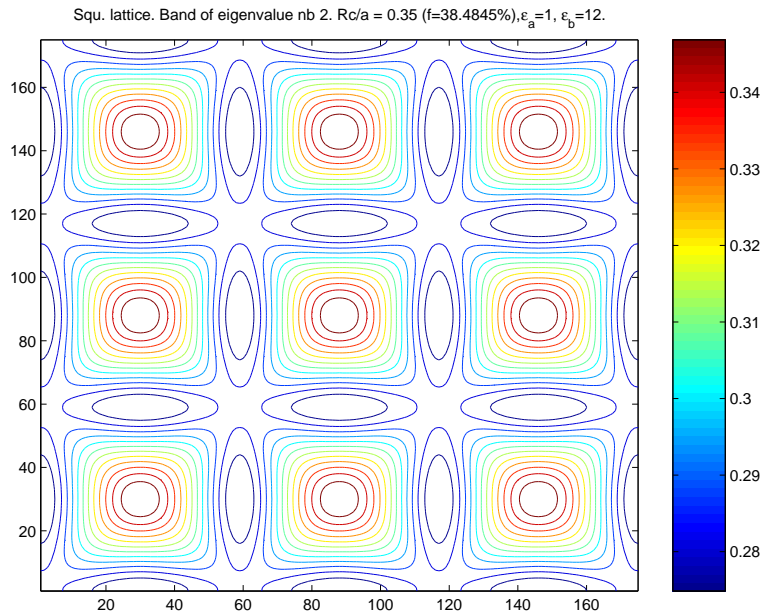


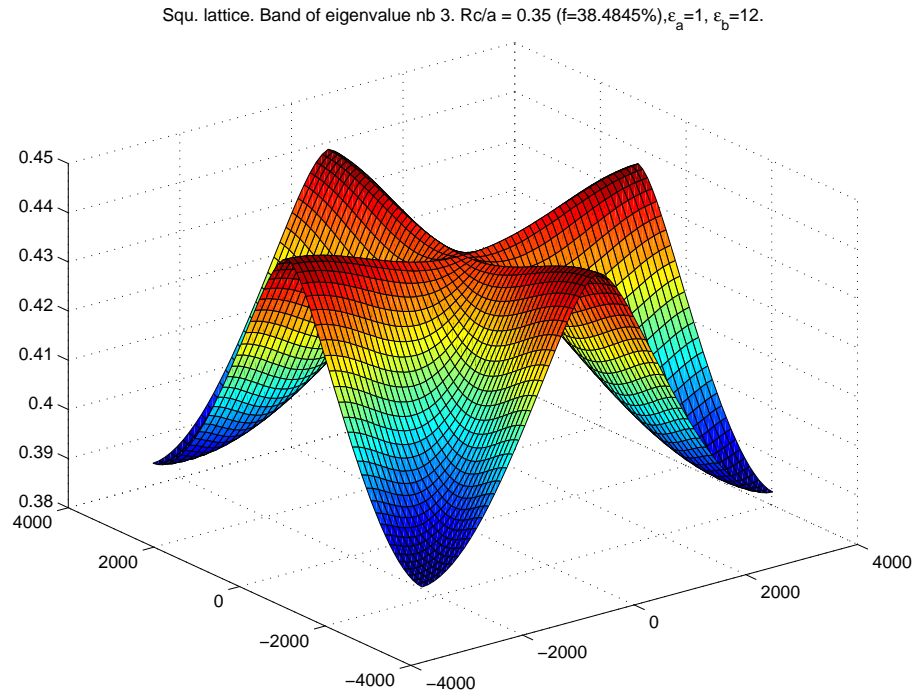
Figure 5: k -surfaces for the first eigenvalue of the system.



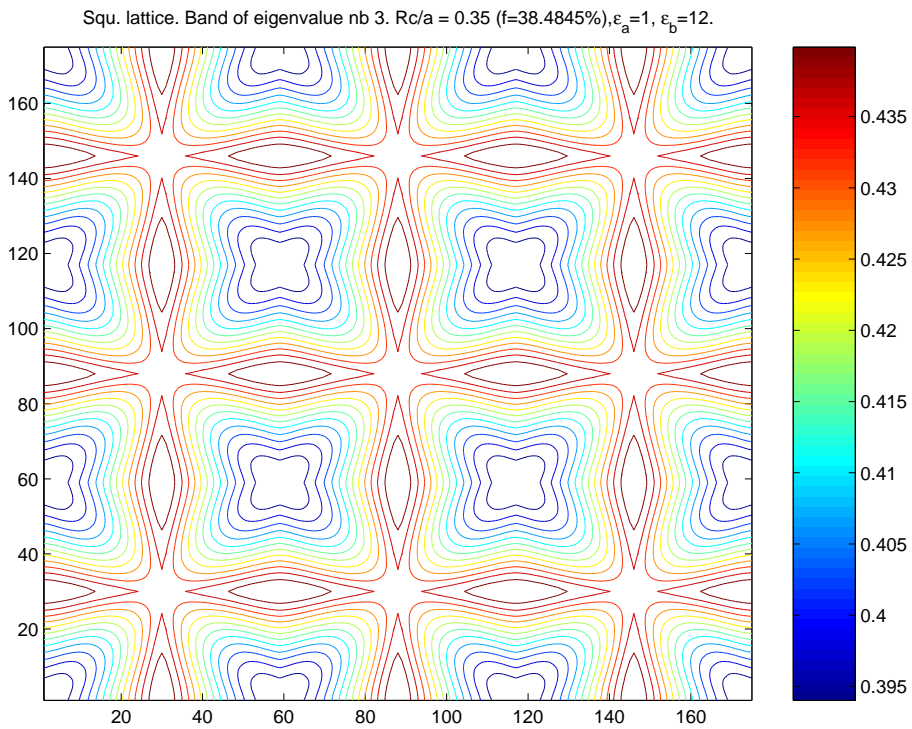
(a) Brillouin cell.

(b) 2D k -surface.**Figure 6:** k -surfaces for the second eigenvalue of the system.

however, because of phase matching, power and phase are in directions that make an angle greater than $\pi/2$. Although it is not necessarily π like in a pure left-handed regime, it is still in the regime of left-handed behavior. Fig. 10 can be completed to see this phenomenon.



(a) Brillouin cell.

(b) 2D k -surface.**Figure 7:** k -surfaces for the third eigenvalue of the system.

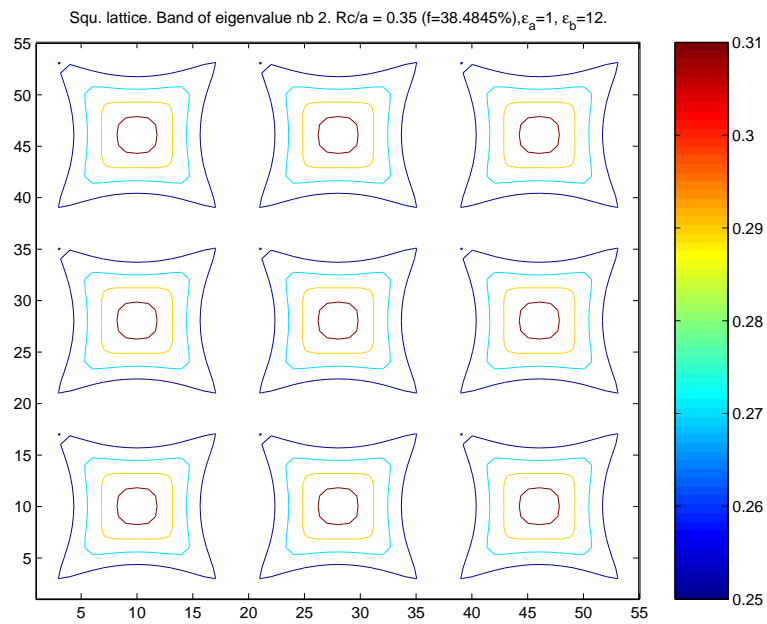


Figure 9: k -surface for the second eigenvalue.

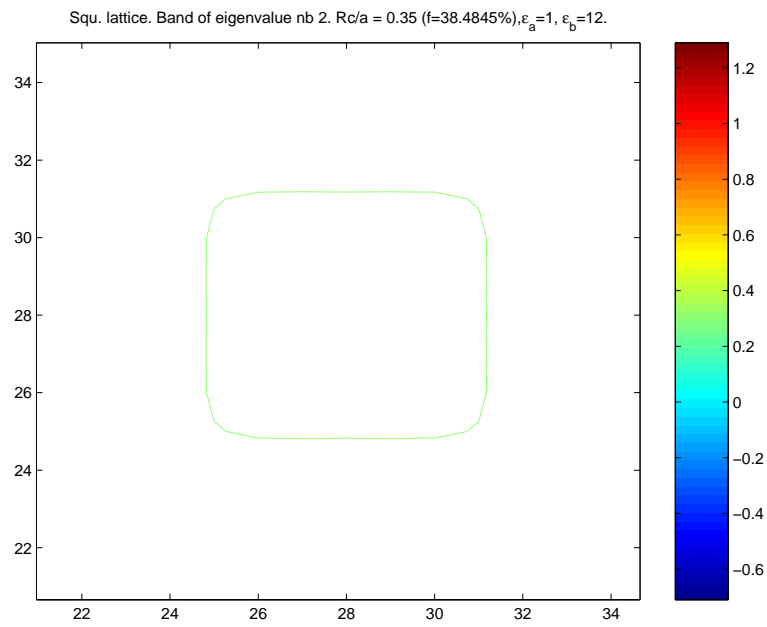


Figure 10: k -surface for the second eigenvalue for the specific frequency where the radius of curvature is positive.